Turk J Elec Eng & Comp Sci, Vol.18, No.5, 2010, © TÜBİTAK
doi:10.3906/elk-0906-14

Precise position control using shape memory alloy wires

Burcu DÖNMEZ[1], **Bülent ÖZKAN**[2], **Suat KADIOĞLU**[3]
[1] *The Scientific and Technological Research Council of Turkey, Defense Industries Research and Development Institute (TÜBİTAK-SAGE), P. K. 16, 06261, Mamak, Ankara-TURKEY*
e-mail: bdonmez@sage.tubitak.gov.tr
[2] *The Scientific and Technological Research Council of Turkey, Defense Industries Research and Development Institute (TÜBİTAK-SAGE), P. K. 16, 06261, Mamak, Ankara-TURKEY*
e-mail: bozkan@sage.tubitak.gov.tr
[3] *Middle East Technical University, Mechanical Engineering Department, 06531, Ankara-TURKEY*
e-mail: kadioglu@metu.edu.tr

Abstract

Shape memory alloys (SMAs) are active metallic "smart" materials used as actuators and sensors in high technology smart systems [1]. The term shape memory refers to ability of certain materials to "remember" a shape, even after rather severe deformations: once deformed at low temperatures, these materials will stay deformed until heated, whereupon they will return to their original, pre-deformed "learned" shape [2]. This property can be used to generate motion and/or force in electromechanical devices and micro-machines. However, the accuracy of SMA actuators is severely limited by their highly nonlinear stimulus-response characteristics. In this work, modeling, simulation, and experimental efforts to precisely control the position of a Ni-Ti based shape memory alloy wire is presented. In this content three separate control strategies are tried and very good positioning accuracies are obtained.

Key Words: *Shape memory alloy wire, precise control, smart materials, computer simulations, experiment*

1. Introduction

In recent years, miniaturization has created the need of compact smart material-based actuators to power mechanical devices built at smaller scales. One of the most promising new actuator technologies developed in the last few years are the actuators employing shape memory properties. Actuators based on shape memory alloys (SMA) have a high power to weight ratio and have found applications in many areas including micromechatronics and light robotics.

The shape memory effect in SMA is based on the transition between low temperature martensite phase and the high temperature austenite phase (Figure 1). This phase variation between austenite and martensite induces dimension and shape changes in the material, thus motion can be generated by heating the material (Figure 2). Shape memory materials can either be driven by an outside heat source or by resistive heating created by passing electrical current through them. In actuator applications, especially the latter method, resistive heating, is employed in which the current through the wire can be controlled.

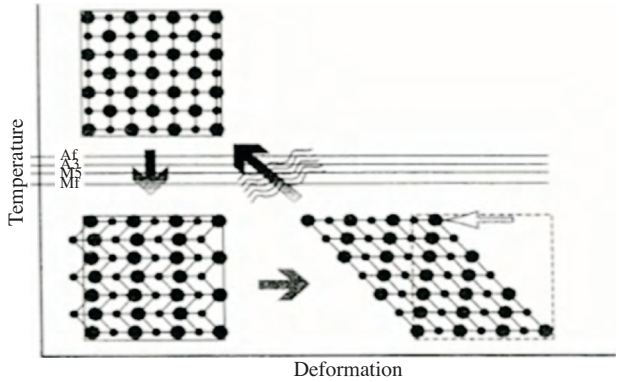

Figure 1. Deformation-temperature diagram for SMA materials.

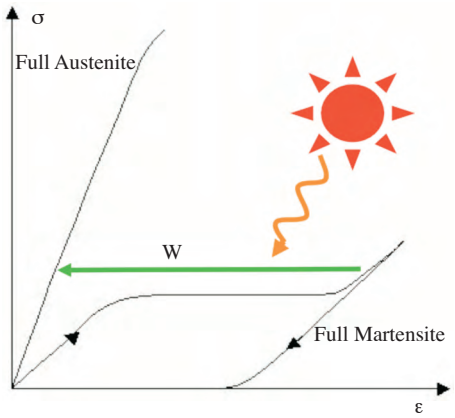

Figure 2. Work extraction from SMAs.

Until recently, SMAs have been used with "on-off" control in electromechanical actuators, because of the intrinsic difficulty in modeling and controlling accurately the phase transition involving the microscopic structural rearrangements, which take place quite sharply and in a highly complex and nonlinear fashion [3]. The main difficulty in controlling these materials is the hysteresis appearing in the phase transition through which they go. One possible solution to this question would imply developing an accurate model for the material thermomechanical behavior; however, formulation of adequate macroscopic constitutive laws is very complex since shape memory behavior depends on stress, temperature and connected with the phase of the material (austenitic or martensitic) and the thermodynamics underlying the transformation process [4].

In the study by Asua et al. [5], the researchers used a classical proportional-integral (PI) controller and a feed-forward loop compensated PI controller to control the SMA wire, where the feed-forward element is

obtained by the neural network approximation of the wire behavior and, respectively, 0.005 and 0.003 mm of positioning accuracies were reported.

Kılıçarslan et al. [6] proposed Adaptive Neuro Fuzzy Inference System (ANFIS) modeling of the SMA wire and used the inverse of this model as a controller obtaining 0.0002 inch (0.005 mm) of positioning accuracy, then a PI controller is also implemented in the system to compensate the errors due to disturbances. Kumagai et al. [7] employed a regular PD controller and then used inverse ANFIS model as a feed-forward element with the PD controller for trajectory tracking problem. They used both the position and velocity data as inputs to the system.

In this work, closed-loop position control studies based on a nickel–titanium alloy (Ni-Ti) SMA wire trained to contract upon heating are discussed. Wire with a load hanging on the tip is heated by controlled electrical current passing through it, creating phase transition and thus contraction is obtained. Proportional-integral, feed-forward loop compensated PI and neural network control strategies have been tested in simulation environment and experimental set-up.

The aim of the present work is to investigate and compare the selected closed loop control strategies applied on an SMA wire in search to accurately control the micro positioning of the wire. In this context, the SMA model derived through identification experiments is also validated by demonstrating that simulations are in very good agreement with the experimental results.

2. Experimental Set-Up

In the experiments, Ni-Ti based shape memory alloy wire 80 mm long with a diameter of 0.2 mm is controlled using the MATLAB© Real Time Windows Target® module. The tests are performed in the experimental set-up consisting of the following elements:

- Mechanical structure
- Specially designed wire grips
- Dead weight
- LVDT (Linear Variable Displacement Transducer) displacement sensor (BALLUFF BTL05)
- Electronic load (DATEL DTL32A-LC)
- Power supply (INSTEK PST3202)
- Current sensor (calibrated ceramic resistance)
- Data acquisition and control card (National Instruments 6036-E)
- Connector block (SCB 68)
- PC

Figure 3 illustrates the schematic representation of the experimental test bench designed to perform electro-thermomechanical characterization of thin SMA wires. The wire is secured between the grips and the lower end is attached to the moving element of the LVDT. The wire is loaded by hanging a dead weight to assure uniaxial tensile stress state on the SMA wire.

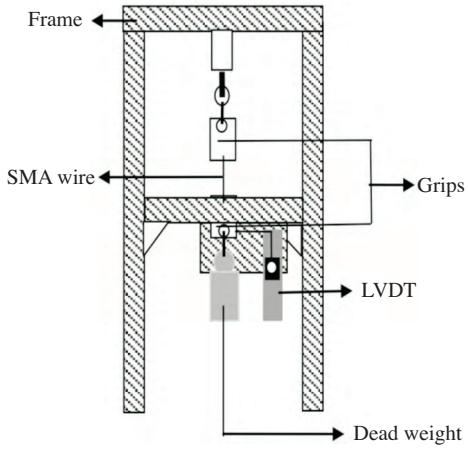

Figure 3. Schematic view of the characterization test bench.

The displacement of the SMA is measured by the LVDT with system resolution less than 0.1 mV and full scale reading is 10 Volts. The current supplied to the wire by the power supply is controlled using the computer, control card, and the electronic load. The control computer generates and supplies the necessary voltage to adjust the resistance of the electronic load which is connected to the SMA wire in series so as to control the current through the circuit (Figure 4).

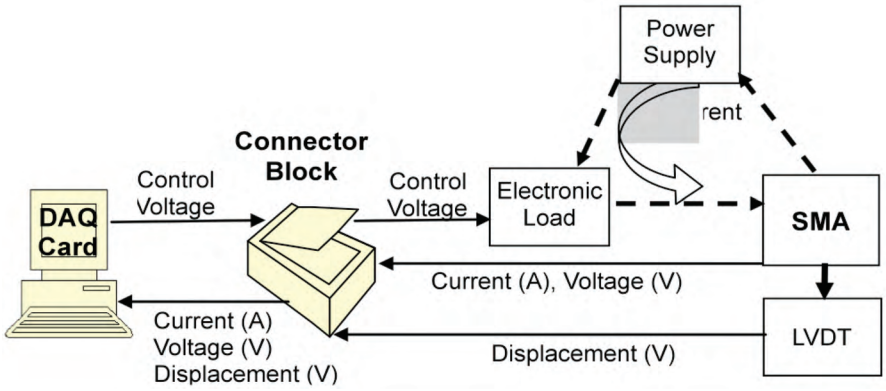

Figure 4. Schematic view of data acquisition and control system set-up.

The current passing through the wire, generated voltage, and displacement data are collected using the data acquisition card at a rate of 100 Hz. The data obtained are processed in real time using MATLAB© SIMULINK®, and the noise is eliminated using a discrete filter of second order with a cut-off frequency of 5 Hz.

3. Modeling

In the first stage, current-contraction characterization of the wire is performed using the set-up. For characterization purpose the current profile is applied to the wire under 140 MPa stress up to 600 mA, as given in Figure 5, and the contraction-current plot is obtained as shown in Figure 6.

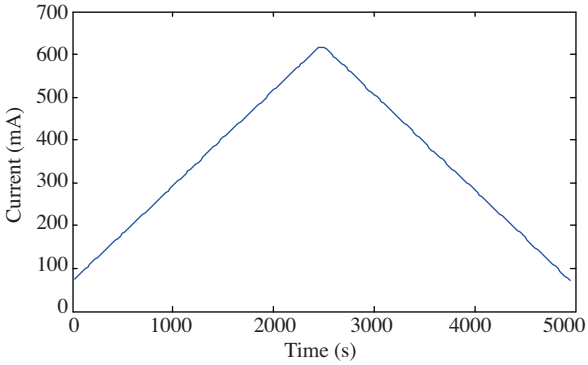

Figure 5. Current profile supplied for characterization.

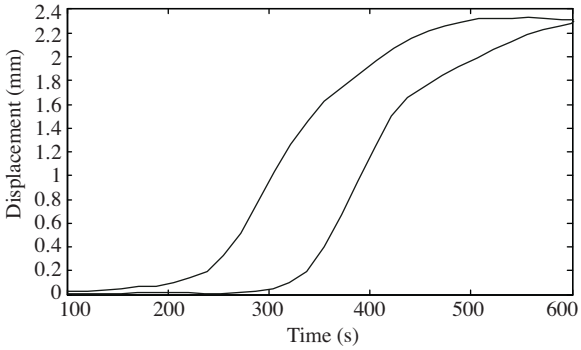

Figure 6. Contraction vs. current plot.

In order to generalize the study, in modeling of the wire, absolute strain is used as the variable instead of contraction. Using the data acquired in the characterization tests strain-current and absolute strain-current plots are obtained as shown in Figure 7 and Figure 8, respectively. Then, absolute strain-current relation of the wire is modeled by curve fitting using sigmoid type functions. The equations modeling the heating and cooling curves are

$$\varepsilon = \varepsilon_l \left[1 - \frac{1}{1 + e^{(-a_M (I_M - I))}} \right] \tag{1}$$

$$\varepsilon = \varepsilon_l \left[1 - \frac{1}{1 + e^{(-a_A (I - I_A))}} \right] \tag{2}$$

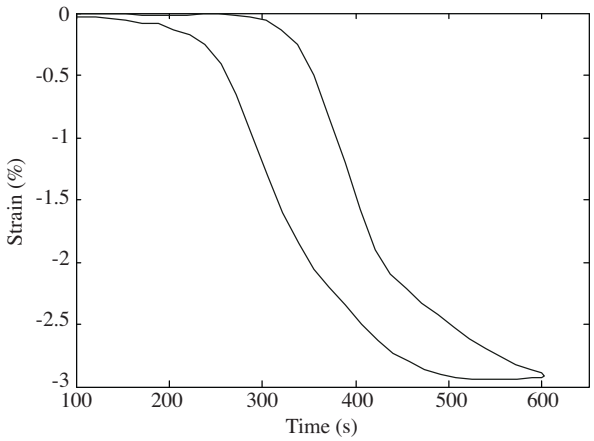

Figure 7. Strain vs. current plot.

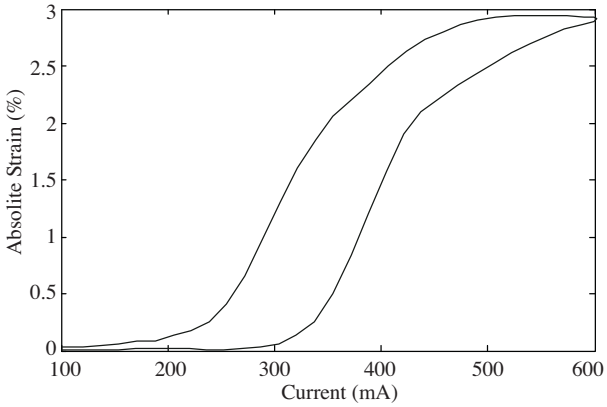

Figure 8. Absolute strain vs. current plot.

In the above relationships, firstly, the values for the variables martensite start m_s, martensite finish m_f, austenite start a_s, austenite finish a_f currents, and maximum recoverable strain (ε_l) are obtained, then the parameters used in the models are found as

$$a_A = 5/(a_s - a_f) \qquad a_M = 5/(m_s - m_f)$$

$$I_A = 0.5(a_s + a_f) \qquad I_M = 0.5(m_s + m_f).$$

The model obtained for absolute strain-current together with the respective experimental data is shown in Figure 9.

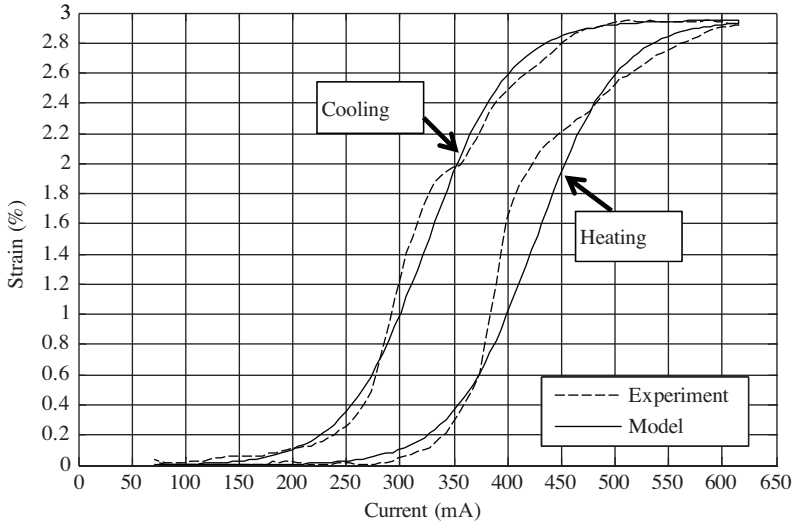

Figure 9. Absolute strain-current model.

4. Simulations and tests

In the control system design to control the strain of the SMA wire, some researchers have chosen to greatly simplify the material's behavior by creating a model where the phase transition temperature is single and same for heating and cooling by completely ignoring the effects of the large hysteresis [8]. In this study, the controller design studies begin with modeling the SMA wire with simple linear models. The calculated parameters are then used to control the non-linear realistic model in the simulations and in the experiments on the test set-up.

4.1. Proportional-integral control method

In the first stage, a control system is designed regarding the widely used proportional-integral type controller due its straightforward application [9]. In this type of controller, the control signal to be sent to the plant, or the system to be controlled, is generated by multiplying the error between the desired and actual values of the strain and sum of the error within a certain interval with the proportional (P) and integral (I) gains, respectively.

Using the block diagram presented in Figure 10 for PI-type controller the following relations can be obtained:

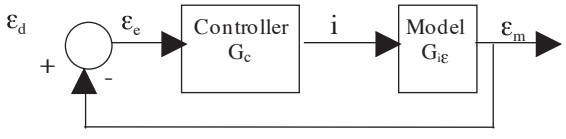

Figure 10. Block diagram for PI-type controller.

$$\varepsilon_m = \varepsilon_e.G_c(S).G_{i\varepsilon}(s) \tag{3}$$

$$\varepsilon_e = \varepsilon_d - \varepsilon_m \tag{4}$$

$$\varepsilon_m = (\varepsilon_d - \varepsilon_m)G_{\cdot c}(s).G_{i\varepsilon}(s) \tag{5}$$

In the diagram, i is the current; ε_d, ε_m, and ε_e represent the desired strain, measured strain, and strain error, respectively; G_c and $G_{i\varepsilon}$ represent the controller and model transfer functions.

Using the block diagram algebra, the overall transfer function of the closed-loop control system can be obtained from the previous expressions as given in equation (6).

$$G_s(s) = \frac{\varepsilon_m}{\varepsilon_d} = \frac{G_c(s).G_{i\varepsilon}(s)}{1 + G_c(s).G_{i\varepsilon}(s)} \tag{6}$$

If a simple linear model as ε=K1$\cdot$i is assumed for the strain-current model seen in Figure 11, the plant transfer function is obtained simply as $G_{i\varepsilon}$=K_1. Also, the transfer function for PI control block is as given in equation (7).

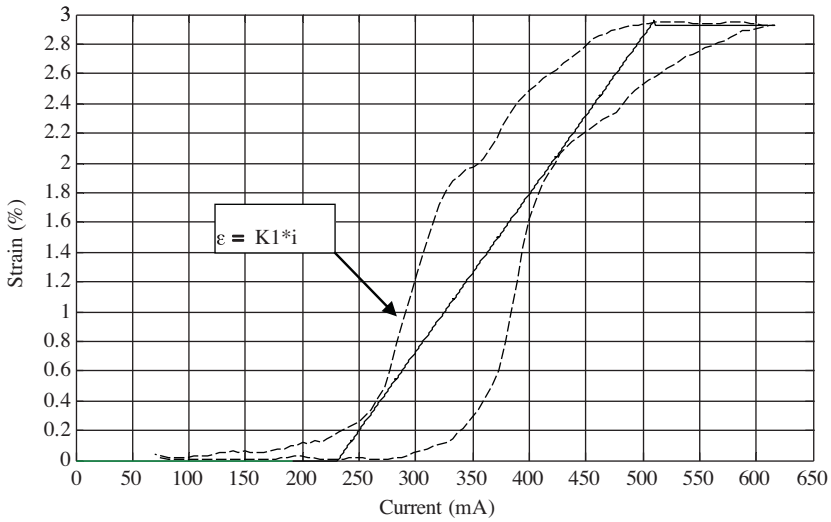

Figure 11. Linear strain-current model.

$$G_c(s) = K_p + \frac{K_i}{s} = \frac{K_p.s + K_i}{s} \tag{7}$$

where K_p and K_i denote the proportional and integral gains of the controller.

Using G_c(s), the system transfer function between the desired and measured strain values then becomes

$$G_s(s) = \frac{\varepsilon_m}{\varepsilon_d} = \frac{G_c(s).G_{i\varepsilon}(s)}{1 + G_c(s).G_{i\varepsilon}(s)} = \frac{K_1K_p.s + K_1K_i}{(K_1K_p + 1)s + K_1K_i} \tag{8}$$

The controller parameters can be tuned using various techniques. In this context, one of the most frequently used techniques is pole-placement of closed loop transfer function. According to this technique,

poles can be placed using specified polynomials, such as Butterworth and Chebyschev polynomials. These polynomials can be used to place the poles of the closed loop system to make the system stable with the required bandwidth. The system response obtained using Butterworth polynomials is generally observed to be better than the response using Chebyschev polynomials, thus in this design Butterworth polynomials are used [10].

When the closed loop characteristic polynomial is equated to first order Butterworth polynomial equation, we obtain

$$\frac{(K_1.K_p+1)}{K_1.K_i}.s+1=\frac{s}{\omega_c}+1 \tag{9}$$

The proportional gain K_p of the controller is chosen to be 300 considering that nearly 300 mA current is needed to nullify a strain error of 1% in the linear model, and the bandwith ω_c is selected to be 0.05 Hz. Using these values the integral gain (K_i) is calculated as 55.

Using the calculated controller parameters simulations are run on the non-linear model and tests are performed with step commands. The simulation and test results with the commands can be seen in Figure 12. As can be understood from the detailed plot presented in Figure 13, the command is followed with approximately 0.005% error in strain.

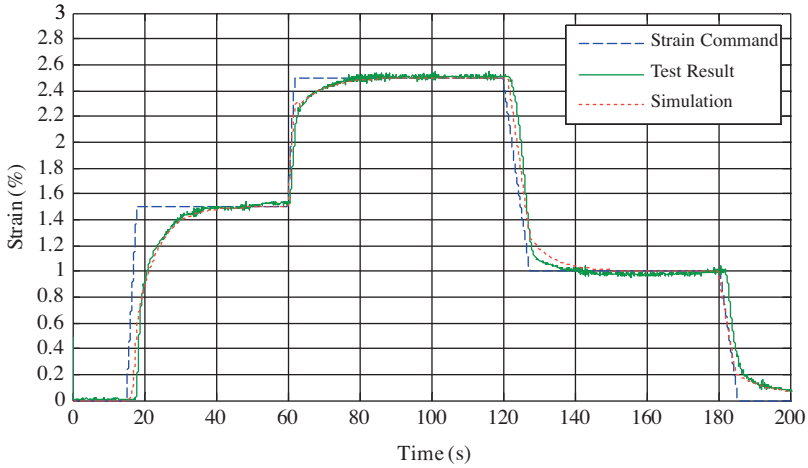

Figure 12. Test and simulation results of the system with PI-type controller.

4.2. Feed-forward loop compensated proportional-integral control method

In this control scheme, an inverse model for current-strain relation is obtained for heating and cooling states of the wire using curve fitting toolbox of MATLAB® as two polynomials for heating and cooling (Figure 14). Then, this model is integrated to the control system as given in Figure 15, the current command from the feed-forward loop is adjusted using the gain block to avoid overshooting of the response, and the remaining error is suppressed by the PI controller.

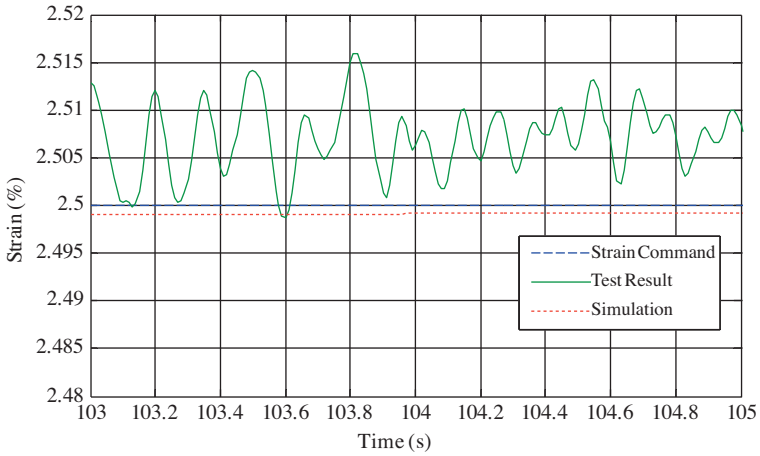

Figure 13. Detailed view of test and simulation results of the system with PI-type controller.

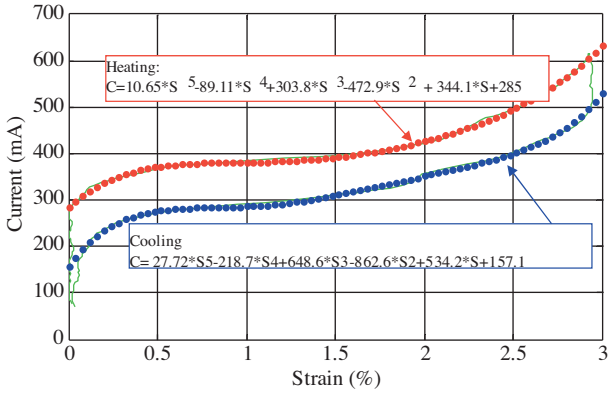

Figure 14. Inverse strain-current model.

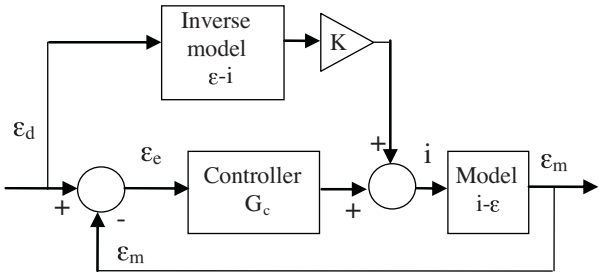

Figure 15. Block diagram of feed-forward loop compensated PI-type control.

Simulations were run in SIMULINK® environment and tests were performed using the previously computed controller gains of K_p=300, K_i=55, and the feed-forward gain of K=0.8. When the results presented in Figure 16 are compared to the results with regular PI controller the response time is observed to be shorter for PI controller with feed-forward loop using the same controller parameters. Using this control scheme also approximately 0.005% strain control accuracy can be achieved as seen in Figure 17.

4.3. Neural network control method: narma-l2 controller

In this portion of the study, the position of the SMA wire is controlled by a neural network (NN) control scheme. NNs are well known for their capability of approximating nonlinear mappings to any desired accuracy [5]. Their properties make them invaluable tools for solving nonlinear control problems. In this context, since an analytical description of the SMA behavior is not easily obtainable, NN can be used to learn the model of the SMA characteristics by means of several sets of experimental input–output mappings measured using the experimental set-up. The implemented NN controller is NARMA-L2 which is a built-in controller in MATLAB® SIMULINK®, Neural Network Toolbox™ blockset [11].

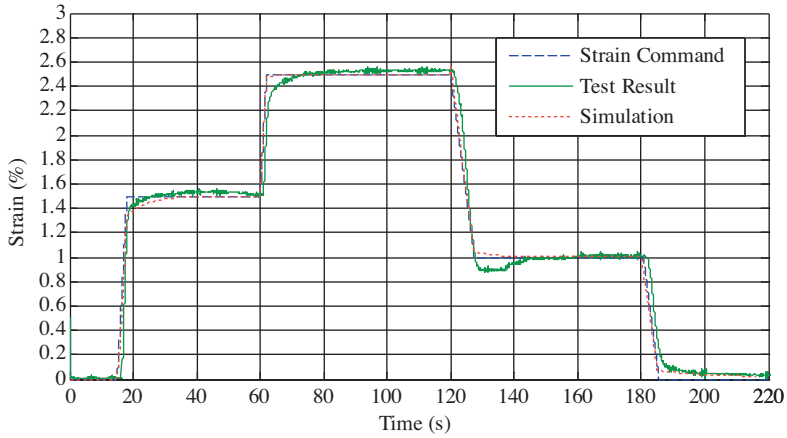

Figure 16. Test and simulation results of the system with feed-forward loop compensated PI-type controller.

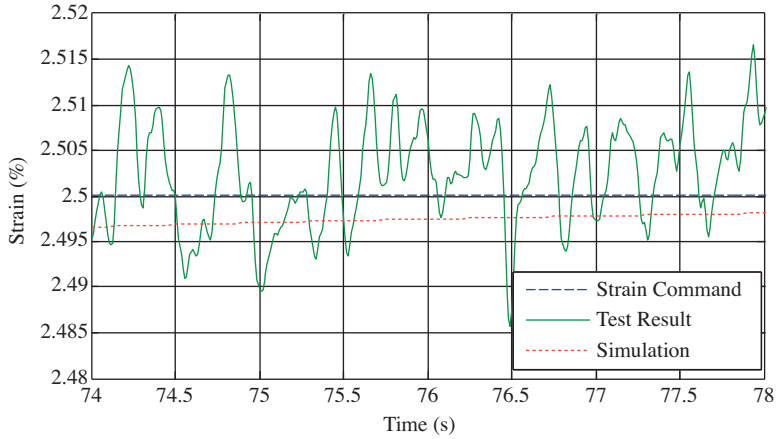

Figure 17. Detailed view of test and simulation results of the system with feed-forward loop compensated PI-type controller.

Typically, neural networks are adjusted, or trained, so that a particular input leads to a specific target output. A lot of input/target pairs, i.e. input and output data sets are needed to train a network. 30000 pairs of current-strain data are used to train the NN. The NN controller proposed in this work (Figure 18) learns off-line the dynamics of the system using the Levenberg–Marquardt (L-M) algorithm (implemented in Matlab as function trainlm), which was designed to approach second-order training speed without having to compute the Hessian matrix like Quasi-Newton methods. The Levenberg–Marquardt algorithm uses this approximation to the Hessian matrix in the Newton-like update

$$x_{k+1} = x_k - \left[J^T J + \mu I\right]^{-1} J^T e, \tag{10}$$

where J is the Jacobian matrix that contains first derivatives of the network errors with respect to the weights (x_k).

When the scalar μ is zero, this is just Newton's method, using the approximate Hessian matrix. When μ is large, this becomes gradient descent with a small step size.

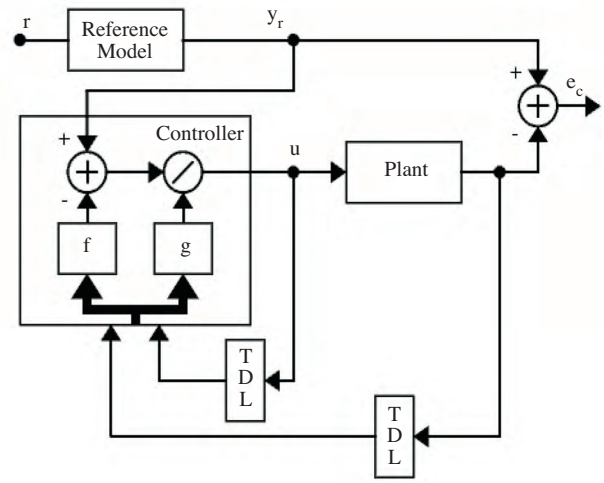

Figure 18. Block diagram of the NARMA-L2 controller [12].

The number of hidden layers to be employed is determined by the convergence study performed on the performance index of the L-M training algorithm by using the data acquired during the characterization tests. The performance index is based on the minimization of the mean square error with gradient descent optimization procedure. The number of layers determines the accuracy of the controller, however, as the number of hidden layers grows the computation time for each step increases. Figure 19 shows the convergence curve for the performance index obtained using different number of layers. As can be seen from the plot, the index seems to converge after 5 layers. Thus, 5 hidden layers are chosen to be used in the model.

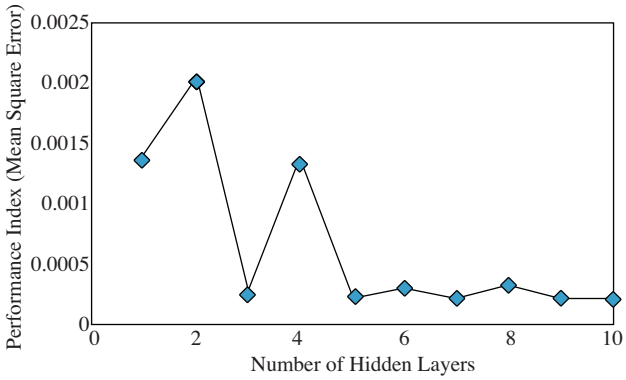

Figure 19. Performance index with respect to number of hidden layers.

The input layer of the NN receives two successive samples of the desired contraction signal and the output layer gives the estimated value of the necessary current that must be applied to the wire in order to obtain the desired contraction. In the employed NN scheme 1000 iterations have been found necessary to achieve a minimum of the error term.

Narma-L2 controller is integrated to the control system as given in Figure 20, then the simulations are made and tests are conducted. Test and simulation results are presented in Figure 21.

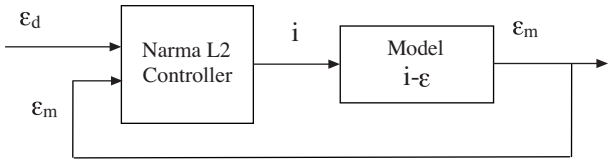

Figure 20. Block diagram of the system with Narma-L2 controller.

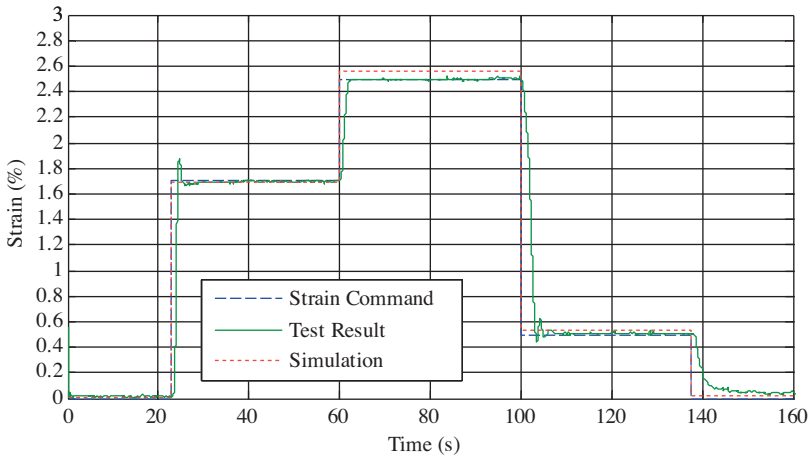

Figure 21. Test and simulation results of the system with NN Narma-L2 controller.

As can be seen in the detailed plot presented in Figure 22 with this type of controller although small and quickly damped overshoots are observed strain of the wire can be controlled with an accuracy of 0.005 %.

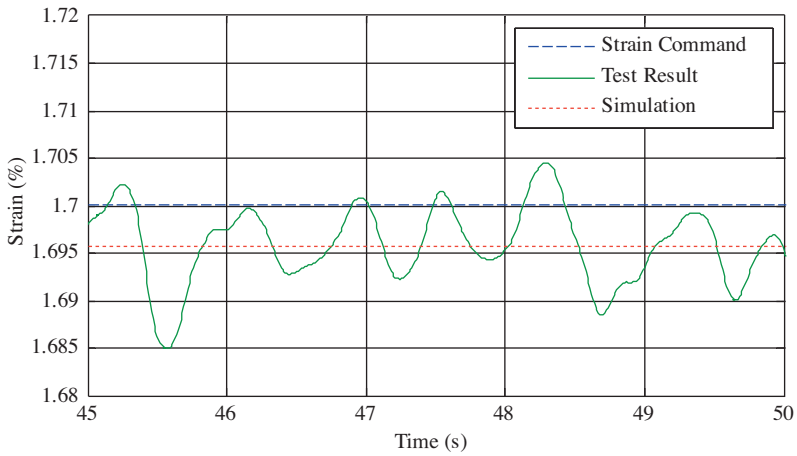

Figure 22. Detailed view of test and simulation results of the system with NN Narma-L2 controller.

5. Conclusions

Shape memory alloys are materials whose dimensions can be modified due to a temperature-dependent structural phase transition. This property can be used to generate motion or force in electromechanical devices and micro-machines. However, they have traditionally been used as "on-off" electromechanical actuators, mainly

because of the difficulty in accurately controlling the martensite-austenite proportion due to the fact that the microscopic rearrangements involved in the structural changes take place quite sharply and in a highly complex and nonlinear fashion with the hysteresis appearing in the phase transition. In this work, despite all the complications due to the phase transition, through simulations and experiments, it is proved that shape memory alloy wires can be used successfully in micro-positioning applications. Simulations are run and tests are conducted using proportional-integral, feed-forward compensated proportional-integral type control and neural network controller.

The parallelism between the simulations and tests confirms the correctness of the developed model. If the employed systems are investigated for their steady state error performances it can be concluded that all methods give approximately the same results. The obtained 0.005% steady state error means a 0.005 mm of positioning error in a 100 mm length of wire. This error can be reduced by using more accurate position sensors. When the control systems are compared for their speed of response it can be observed that best results are achieved with Narma-L2 controller.

In Figure 23, the test performed using Narma-L2 controller with sinusoidal strain command is presented.

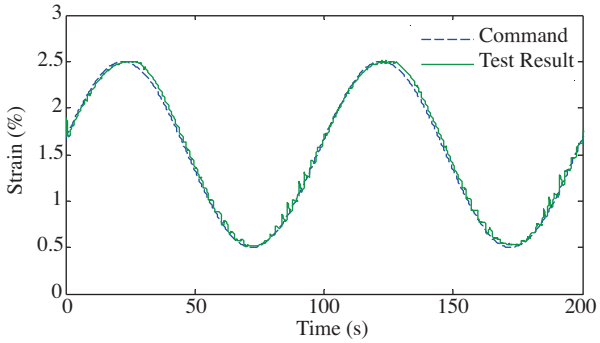

Figure 23. Test results with sinusoidal command using Narma-L2 controller.

The simulations and the tests show that shape memory alloys can seriously be considered as a positioning actuator in micro-machines and the proposed control strategies can be used in controlling the developed actuators since they lead to good positioning accuracies and consistent with the results presented in the literature [5], [6]. Also, the inverse SMA model in forms of polynomials as used in this study is a simpler approach to obtain and implement when compared to NN based feed-forward elements presented in the literature with less on-line and off-line computation costs.

As a future work of this study, research can be conducted on control of SMAs employing their self-sensing capabilities and force feedback control using SMAs as the active element.

References

[1] C.M. Wayman, T.W. Duerig, K.N. Melton, An Introduction to Martensite and Shape Memory, Engineering Aspects of Shape Memory Alloys, Butterworth-Ileinemann, 1990.

[2] T.W. Duerig, "Applications of shape memory, martensitic transformations", Materials Science Forum, pp. 679-692, 1990.

[3] K. Ikuta, "Micro/miniature shape memory alloy actuator", Proceedings of IEEE Conference on Robotics and Automation, pp. 2156-2161, 1990.

[4] D. Reynearts, Brussels H., "Design aspects of shape memory actuators", Mechatronics, Vol. 8, pp. 635-656, 1997.

[5] E. Asua et al., "Neural network-based micropositioning control of smart shape memory alloy actuators", Engineering Applications of Artificial Intelligence, Vol. 24, pp. 796-804, 2008.

[6] A. Kılıçarslan et al., "ANFIS Based Modeling and Inverse Control of a Thin SMA Wire", Modeling, Signal Processing, and Control for Smart Structures, Proceedings of SPIE, Vol. 6926, 2008.

[7] A. Kumagai, T. Liu, and P. Hozian, "Control of shape memory alloy actuators with a neuro-fuzzy feed-forward model element", Journal of Intelligent Manufacturing, Vol. 17, 2006.

[8] J.L. Pons, D. Reynaerts, J. Peirs, R. Ceres, H. VanBrussel, "Comparison of different control approaches to drive SMA actuators", ICAR'97, 1997.

[9] B. Kuo, Automatic Control Systems, Prentice-Hall Inc., 1995.

[10] R.W. Erickson, Filter Circuits, ECEN2260, 1997.

[11] K.S. Narenda, S. Mukhopadhyay, "Adaptive control using neural networks and approximate models", IEEE Transactions on Neural Networks, Vol. 1, pp. 4-27, 1990.

[12] MATLAB, "Neural Network Toolbox, Narma-L2 Controller", The Mathworks Inc., 2007.

[13] K. Lei, Y. Yam "Modeling and experimentation of a positioning system of SMA wires", Smart Structures and Materials 2000: Sensory Phenomena and Measurement Instrumentation for Smart Structures and Materials, Proceedings of SPIE, Vol. 3986, 2000.

[14] A. Nespoli, et al. "The high potential of shape memory alloys in developing miniature mechanical devices: A review on shape memory alloy mini-actuators", Sensors and Actuators A: Physical, Vol. 158, pp. 149-160, 2010.